Molecular Biology of the Cell
Vol. 12, 981–995, April 2001

Identification of Discrete Classes of Endosome-derived Small Vesicles as a Major Cellular Pool for Recycling Membrane Proteins

Seong-Nam Lim,[*†] Frank Bonzelius,[†#] Seng Hui Low,[‡‖] Holger Wille,[§] Thomas Weimbs,[‡‖] and Gary A Herman[*†¶]

[*]Department of Pediatrics, Division of Gastroenterology and Nutrition, [†]The Hormone Research Institute, [‡]Department of Anatomy, and [§]Department of Neurology University of California, San Francisco, San Francisco, California 94143

Submitted October 2, 2000; Revised January 3, 2001; Accepted January 24, 2001
Monitoring Editor: Suzanne R. Pfeffer

Vesicles carrying recycling plasma membrane proteins from early endosomes have not yet been characterized. Using Chinese hamster ovary cells transfected with the facilitative glucose transporter, GLUT4, we identified two classes of discrete, yet similarly sized, small vesicles that are derived from early endosomes. We refer to these postendosomal vesicles as endocytic small vesicles or ESVs. One class of ESVs contains a sizable fraction of the pool of the transferrin receptor, and the other contains 40% of the total cellular pool of GLUT4 and is enriched in the insulin-responsive aminopeptidase (IRAP). The ESVs contain cellubrevin and Rab4 but are lacking other early endosomal markers, such as EEA1 or syntaxin13. The ATP-, temperature-, and cytosol-dependent formation of ESVs has been reconstituted in vitro from endosomal membranes. Guanosine 5′-[γ-thio]triphosphate and neomycin, but not brefeldin A, inhibit budding of the ESVs in vitro. A monoclonal antibody recognizing the GLUT4 cytoplasmic tail perturbs the in vitro targeting of GLUT4 to the ESVs without interfering with the incorporation of IRAP or TfR. We suggest that cytosolic proteins mediate the incorporation of recycling membrane proteins into discrete populations of ESVs that serve as carrier vesicles to store and then transport the cargo from early endosomes, either directly or indirectly, to the cell surface.

INTRODUCTION

Proteins internalized via receptor-mediated endocytosis are rapidly transported via clathrin-coated vesicles to endosomal structures located in the periphery of the cell known as early or sorting endosomes (Gruenberg and Maxfield, 1995; Mellman, 1996; Clague, 1998). From there, ligands and their cognate receptor as well as fluid material are delivered via late endosomes to lysosomes where they are degraded. Some of the receptors, including the transferrin (Tf) receptor (TfR), are recycled back to the cell surface from the peripheral endosomes, either directly or indirectly, via pericentriolar recycling endosomes.

One of the unsolved issues is the mechanism by which those plasma membrane proteins that are not degraded are transported out of the sorting endosomes. It is not clear whether the transport vehicles are tubules or vesicles. It is also not known in molecular terms how recycling membrane proteins are sorted from each other in the sorting endosome. For example, there is evidence that membrane proteins are transported to the recycling endosomes by default, following the bulk flow of lipids (Mayor *et al.*, 1993). On the other hand, there has been circumstantial evidence to support a role for coated vesicles in the recycling of these proteins from endosomes. A number of coat proteins copurify with fractions enriched in early endosomes (Whitney *et al.*, 1995). Electron microscopic studies also demonstrate budding profiles on endosomes, many containing clathrin and other coat proteins (Stoorvogel *et al.*, 1996; Futter *et al.*, 1998). Endo-

Present addresses: [¶]Department of Cell Biology, Lerner Research Institute, The Cleveland Clinic Foundation, Cleveland, OH 44195; [#]Abteilung Biologie für Mediziner, Zoologisches Institut der J.W. Goethe-Universität, Theodor-Stern-Kai 7/Haus 75, D-60590 Frankfurt, Germany.

[¶] Corresponding author and present address: Merck Research Laboratories, RY 33-672, Rahway, NJ 07065; e-mail: Gary_Herman@Merck.com.

Abbreviations used: BFA, brefeldin A; BSA, bovine serum albumin; CHO, Chinese hamster ovary; ESV, endocytic small vesicle; GST, glutathione *S*-transferase; GTPγS, guanosine 5′-[γ-thio]triphosphate; Ig, immunoglobulin; IRAP, insulin-responsive aminopeptidase; NEM, *n*-ethyl maleimide; PBS, phosphate-buffered saline; PIP2, phosphatidylinositol 4,5-biphosphate; PLD, phospholipase D; Tf, transferrin; TfR, transferrin receptor.

somes from specialized neuroendocrine PC12 cells have also been shown to give rise to a subset of synaptic vesicles (Faúndez *et al.*, 1997, 1998; Lichtenstein *et al.*, 1998; de Wit *et al.*, 1999).

To explore mechanisms of sorting and transport from early endosomes, we set out to reconstitute endosomal trafficking in vitro. To develop a methodology, we took advantage of several earlier findings. One is that the facilitative glucose transporter, GLUT4, a recycling plasma membrane protein, accumulates within a homogeneous population of small vesicles in primary adipose and muscle cells (James *et al.*, 1987; Rodnick *et al.*, 1992; Herman *et al.*, 1994; Kandror *et al.*, 1995) and in transfected cell types (Herman *et al.*, 1994). In transfected Chinese hamster ovary (CHO) cells, these vesicles are enriched in the insulin-responsive aminopeptidase (IRAP) (Müller, unpublished data), an endogenous plasma membrane protein and marker of GLUT4-containing vesicles in fat and muscle cells (Kandror and Pilch, 1994; Keller *et al.*, 1995; Ross *et al.*, 1996; Aledo *et al.*, 1997; Martin *et al.*, 1997). A second finding is that GLUT4-containing vesicles can be labeled from the surface in cells transfected with epitope-tagged GLUT4 (Wei *et al.*, 1998). Kinetic experiments suggest that these small vesicles are in fact postendosomal long-lived transport vesicles. Finally, we observed that at 15°C surface-labeled GLUT4 or transferrin is internalized into peripheral endosomes but not into small vesicles, thus providing a way to selectively label donor endosomes to be used in cell-free transport assays (Wei *et al.*, 1998). Interestingly, by confocal immunofluorescence at the reduced temperature, internalized GLUT4 and TfR label discrete peripheral endosomal structures. These data suggest that these membrane proteins may transit through discrete subdomains of the same endosome or via physically separate endosomes and that it is worthwhile to compare the behavior of both proteins (Wei *et al.*, 1998).

Here, with improved homogenization conditions, we report the identification of two discrete populations of small, early endosome-derived vesicles that contain either the TfR or GLUT4 and IRAP in transfected CHO cells. To our surprise, we find that these vesicles are quite abundant, containing a significant proportion of the recycling membrane proteins at steady state. We have termed these vesicles endocytic small vesicles (ESVs). We have developed a cell-free assay that reconstitutes the ATP-, temperature-, and cytosol-dependent formation of both classes of ESVs from labeled endosomes but not from labeled plasma membranes, validating the endosomal origin of the vesicles. Our findings suggest that ESVs are vesicular intermediates involved in the transport and/or storage of recycling plasma membrane proteins from endosomes. In addition, the in vitro assay shows that it is possible to perturb the delivery of one cargo protein, GLUT4, without impairing the sorting of others.

MATERIALS AND METHODS

Reagents and Antibodies

Cell culture media and reagents were obtained from the University of California, San Francisco, Cell Culture Facility (San Francisco, CA), with the exception of fetal bovine serum, which was from Life Technologies (Gaithersburg, MD). Enhanced chemiluminescence reagents and ^{125}I were from Amersham (Arlington Heights, IL). Iodogen and dimethylpimelimidate were from Pierce (Rockford, IL). Protein G-Sepharose was from Pharmacia Biotech (Piscataway, NJ). ATP, guanosine 5′-[γ-thio]triphosphate (GTPγS), GTP, brefeldin A (BFA), creatine phosphate, creatine kinase, and bovine serum albumin (BSA) were from Boehringer-Mannheim (Indianapolis, IN). All other reagent-grade chemicals were from Sigma (St. Louis, MO) or Fisher Chemical (Santa Clara, CA). Female Sprague Dawley rats were from Bantin and Kingman (Fremont, CA). The following antibodies were generously provided: monoclonal anti-GLUT4 tail (1F8) (Paul Pilch, Boston University, Boston, MA); polyclonal anti-GLUT4 (Samuel Cushman, National Institutes of Health, Bethesda, MD); monoclonal anti-myc (9E10) (Michael Bishop, University of California, San Francisco, San Francisco, CA); polyclonal anti-IRAP (Susanna Keller, Dartmouth University, Hanover, NH); monoclonal anti-TfR (H68.4) (Ian Trowbridge, Salk Institute, La Jolla, CA); and polyclonal anti-cellubrevin (Reinhard Jahn, Max-Planck-Institute, Heidelberg, Germany). The following antibodies were purchased: polyclonal anti-GLUT4 (R820) (East Acres Biologicals, Cambridge, MA); anti-Rab4, anti-Rab11, anti-EEA1 (Transduction Laboratories, San Diego, CA); and HRP- (Jackson Immunoresearch Laboratories, West Grove, PA) and gold-conjugated secondary antibodies (Pelco, Redding, CA).

Cell Culture

Wild-type and transfected CHO cells were grown as described previously (Wei *et al.*, 1998). Experiments were performed using CHO cells stably transfected with GLUT4 containing a c-myc epitope tag in the first exofacial domain (CHO/G4myc) (Kanai *et al.*, 1993).

Iodination of Anti-myc Antibodies and Transferrin

Monoclonal antibody 9E10 was purified from serum-free hybridoma supernatant by protein G-Sepharose affinity chromatography. Human apotransferrin was further purified by Sephacryl S-300 gel filtration and then iron loaded as described before (Yamashiro *et al.*, 1984; McGraw *et al.*, 1987). Aliquots of purified antibody (100 μg) or iron-loaded transferrin were iodinated by Iodogen-mediated coupling (Grote and Kelly, 1996).

Cytosol Preparation

Rat brain cytosol was prepared using Sprague Dawley rats as described by Clift-O'Grady *et al.* (1998). Aliquots of cytosol were quick-frozen in liquid nitrogen for long-term storage at −80°C

Subcellular Fractionation

CHO/G4myc cells were fractionated using a modification of the procedures described previously (Wei *et al.*, 1998). Cells were washed on tissue culture dishes and scraped into a small volume of Bud buffer (38 mM potassium aspartate, 38 mM potassium glutamate, 38 mM potassium gluconate, 20 mM 3-(*N*-morpholino)propanesulfonic acid, pH 7.2, 5 mM reduced glutathione, 5 mM sodium carbonate, 2.5 mM magnesium sulfate; Clift-O'Grady *et al.*, 1998) containing protease inhibitors. Cells were homogenized using a ball-bearing cell cracker from the European Molecular Biology Laboratory, with a clearance of 10 μm. Approximately 1 mg of the homogenate was layered onto 4.5 ml of a 5–25% glycerol gradient over 400 μl of a 50% (wt/vol) sucrose pad and centrifuged at 60,000 × *g* for 75 min. Fractions were collected from the top and counted on a gamma counter or analyzed by SDS-PAGE and Western blot. Separation of ESVs by equilibrium density centrifugation was accomplished by layering peak fractions containing the ESVs onto 10–45% sucrose gradients and centrifuging for 18 h at 183,000 × *g*.

In Vitro Reconstitution of ESVs

Preparation and Labeling of Donor Membranes. Confluent CHO/G4myc cells were washed with ice-cold phosphate-buffered saline

(PBS). The cells were then incubated in F-12 Ham's solution, 3% BSA, and 10 mM HEPES (pH 7.4) containing either 5 μg/ml (10^7cpm/ml) radioiodinated 9E10 or radioiodinated transferrin for 80 min at 15°C. After the radioligand was removed, the cells were washed with ice-cold PBS containing 3% BSA and then with ice-cold PBS. Cells were scraped into 0.5 ml of ice-cold Bud buffer and homogenized using the ball bearing homogenizer. The homogenate was centrifuged for 30 min at 27,000 × *g* to pellet large membranes, including endosomes. The membrane pellet was resuspended in stripping buffer (2.5 M urea, 250 mM sorbitol, 20 mM HEPES, pH 6.8, 5 mM magnesium acetate, 150 mM potassium acetate; Kuehn *et al.*, 1998) and incubated for 15 min on ice. The membranes were then pelleted by centrifugation for 30 min at 27,000 × *g* and resuspended in Bud buffer. This step was repeated once to ensure the removal of any residual urea.

Budding Reaction. Labeled donor membranes (1 mg/ml) were incubated with 2 mg/ml rat brain cytosol, plus an ATP-regenerating system (1 mM ATP, 8 mM creatine phosphate, 5 μg/ml creatine kinase; Clift-O'Grady *et al.*, 1998), in a total reaction volume of 250 μl. The reaction mixture was incubated on ice for 5 min before warming for 10 min at 37°C. All reactions were then placed on ice for 5 min before further analysis. The reaction mixture was layered on top of 5–25% glycerol gradients (Herman *et al.*, 1994) and centrifuged for 75 min at 60,000 × *g*. After velocity sedimentation, fractions were collected from the top and analyzed as described above.

Negative Staining and Electron Microscopy

Standard sample preparation was done on carbon-coated 600-mesh copper grids that were glow discharged for 30 s before use. Samples (5 μl) of glycerol gradient fractions containing the ESVs were adsorbed for 1 min onto the grids and stained with freshly filtered 2% ammonium molybdate. After the samples dried, they samples were viewed in a JEM 100CX II electron microscope (JEOL, Peabody, MA) at 80 kV and a standard magnification of ×20,000. The magnification was calibrated using negatively stained catalase crystals. The external diameter of individual vesicles was measured parallel to one side of each print, independently of the orientation of the vesicle.

Immunogold Labeling

Samples were adsorbed for 1 min onto Formvar-carbon–coated 200-mesh nickel grids and washed with HBS (10 mM Na HEPES, pH 7.4, 150 mM NaCl, 10 mM NaN_3). The grids were blocked for 10 min with 1% BSA in HBS, washed with HBS, and incubated for 19.5 h at 4°C in a humid chamber with a 1:10 dilution of rabbit anti-GLUT4 immunoglobulin (Ig) G (R820) in HBS with 0.1% BSA. The grids were then washed again with HBS/BSA and incubated for 1 h at room temperature with a 1:150 dilution of 10-nm gold-labeled goat anti-rabbit IgG secondary antibody. The grids were then washed twice with HBS, fixed with 2.5% glutaraldehyde for 4 min at room temperature, washed with distilled water, and stained with freshly filtered 2% ammonium molybdate.

Immunoisolation of In Vivo and In Vitro ESVs

Before protein G-Sepharose beads were used, they were blocked with PBS and 2% BSA. Monoclonal antibody 1F8 or nonspecific mouse IgG was coupled to protein G-Sepharose beads using the cross-linker dimethylpimelimidate at a concentration of 2 mg of antibody per 1 ml of beads. In vivo or in vitro generated ESVs were isolated from glycerol gradients and incubated overnight at 4°C with either 1F8- or IgG-coupled beads in Bud buffer plus 2% BSA. The beads were collected by centrifugation in a microcentrifuge for 10 s and washed with Bud buffer. The vesicle proteins were eluted with Laemmli sample buffer.

Electrophoresis and Immunoblotting

Proteins from the glycerol gradient fractions were precipitated with 0.15% sodium deoxycholate and 6% trichloroacetic acid. The resulting pellet was dissolved in Laemmli sample buffer and analyzed by SDS-PAGE followed by Western blot using enhanced chemiluminescence detection as described by Bonzelius *et al.* (1994). Quantification was by optical densitometry using a charge-coupled device camera and National Institutes of Health Image software.

Purification of the Glutathione S*-Transferase (GST)-GLUT4 Tail*

The GST-GLUT4 tail construct was generated by polymerase chain reaction amplification of the cytoplasmic tail of GLUT4 from pCXN2GLUT4myc (Kanai *et al.*, 1993) and subcloned into pGEX3X. The protein was expressed in the *Escherichia coli* strain DH5α. The fusion protein was purified using a glutathione agarose column according to the manufacturer's instructions (Pharmacia). The eluted protein was dialyzed against Bud buffer before use.

RESULTS

TfR, GLUT4, and IRAP Accumulate within Small Vesicles at Steady State

To visualize the small vesicles, we separated membranes on the basis of size using velocity sedimentation (Herman *et al.*, 1994; Wei *et al.*, 1998). We recently learned that, by using our previous homogenization protocol, at least 50% of the total pool of small vesicles is released from the cell during removal of the cells from tissue culture dishes (Müller, unpublished data). These vesicles are enriched in GLUT4 and IRAP. Hence, our previous results potentially underrepresented the degree to which plasma membrane proteins are localized to small vesicles. Here, we have revised our homogenization scheme so that no material is discarded and all the membranes are fractionated simultaneously.

CHO/G4myc cells were removed from dishes into a small volume of buffer and passed through a ball bearing cell cracker. The homogenate was layered onto a glycerol gradient and centrifuged at 60,000 × *g* for 75 min. Because none of the membranes are discarded, we expect a quantitative representation of the distribution of membrane proteins. Figure 1A shows the results of Western blot analysis after velocity sedimentation. The right-hand side represents the bottom of the gradient where large membranes such as endoplasmic reticulum, Golgi, plasma membranes, and endosomes sediment. The left-hand side represents the top of the gradient where smaller organelles and soluble proteins sediment. As in previous studies (Herman *et al.*, 1994; Wei *et al.*, 1998), GLUT4 is localized to slowly sedimenting small vesicles and larger membranes. Optical densitometry indicates that ~45% of the total pool of GLUT4 are localized to small vesicles (Figure 1B). Small vesicles containing TfR can now be visualized. Approximately 17% of the total pool of TfR are cofractionated with small vesicles. The remainder are localized to large membranes, presumably endosomes and plasma membranes. More than 20% of the cellular pool of the IRAP localizes to small vesicles. A majority of the pool of IRAP localizes with large membranes. A small percentage is identified at the top of the gradient, consistent with the behavior of a soluble protein. Although IRAP is an integral membrane protein, the homogenization procedure may fa-

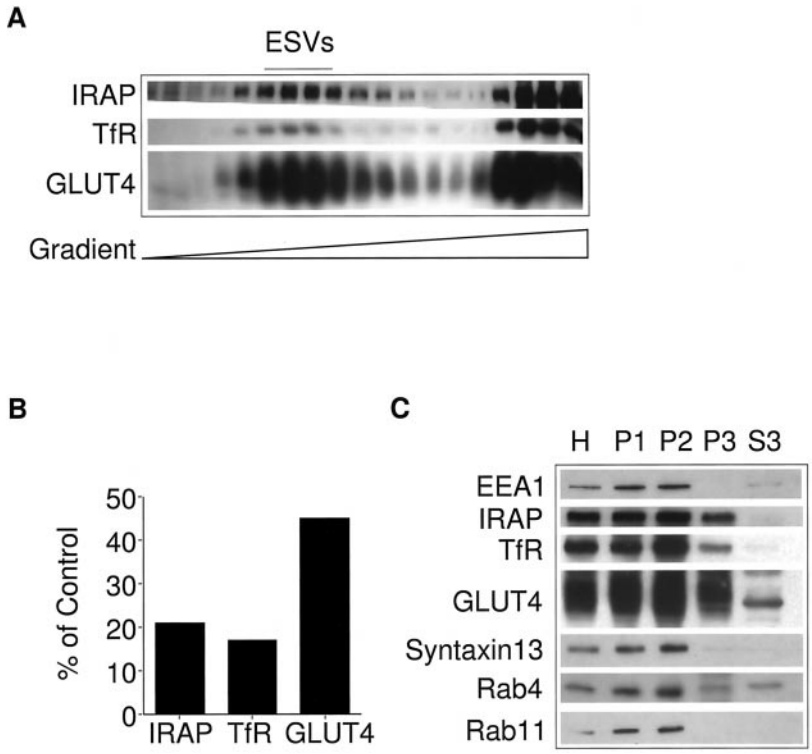

Figure 1. Identification of ESVs in CHO cells stably transfected with myc epitope-tagged GLUT4 at steady state. (A) Western blot analysis of fractions generated by velocity sedimentation. Homogenates from CHO/GLUT4myc cells were fractionated by velocity sedimentation on 5–25% glycerol gradients over a 50% sucrose pad and centrifuged at 60,000 × *g* for 75 min. Note that GLUT4, IRAP, and TfR colocalize with slowly sedimenting small vesicles (fractions 4–12) and larger, rapidly sedimenting membranes at the bottom of the gradient (fractions 15–19). (B) Densitometry analysis of A. For each marker, the total signal was calculated by summing the signal from each fraction. (C) Western blot analysis of fractions generated by differential centrifugation. Each fraction (20 μg) was analyzed: H, homogenate; P1, a pellet centrifuged at 500 × *g* for 5 min (enriched in plasma membranes); P2, a pellet from the supernatant, obtained after a 500 × *g* spin, centrifuged at 27,000 × *g* for 45 min (enriched in endosomal membranes); P3, a pellet from the supernatant left behind by the P2 spin centrifuged at 100,000 × *g* for 1 h (enriched in small vesicles); S3, the supernatant left behind after the P3 spin. Note the inclusion of IRAP, GLUT4, TfR, cellubrevin, and Rab4 but the exclusion of syntaxin13, EEA1, and Rab11 from the small vesicular fractions. A sharp band of ~45 kDa is observed in the S3 fraction. This band, lacking the pattern of the normally glycosylated GLUT4, appears to be a cross-reacting soluble protein and not GLUT4.

cilitate dislocation of the protein from the membranes. We previously observed this phenomenon in the case of the polymeric Ig receptor (Bonzelius *et al.*, 1994). Although it is not known whether IRAP is ubiquitinated, transmembrane proteins degraded by the ubiquitin-proteasome–conjugating system are dislocated from the membranes before degradation (Bonifacino and Weissman, 1998; Plemper and Wolf, 1999). Similar results are obtained when the cells are homogenized using a Teflon-glass homogenizer (Lim, Bonzelius, Low, Wille, Weimbs, and Herman, unpublished observations).

We utilized differential centrifugation to determine whether the small vesicles are enriched for other markers of early endosomes (Figure 1C). Fractions enriched in small vesicles (P3) were compared with fractions enriched in endosomes (P2), plasma membranes and endosomes (P1), or crude homogenate (H). Consistent with the above results, GLUT4, TfR, and IRAP are detected within both endosomal and small vesicular fractions. Although Rabs 4 and 11 are known to be associated with endosomes (Chavrier *et al.*, 1990; van der Sluijs *et al.*, 1992; Ullrich *et al.*, 1996) and Rab4 has been detected within GLUT4-containing membranes (Cormont *et al.*, 1996), only Rab4 was detected within the P3 fraction enriched in small vesicles. The early endosomal marker EEA1 (Mu *et al.*, 1995) is associated with endosomal fractions (P1 and P2) but is absent from the small vesicular fractions. Similarly, the endosomal t-SNARE, syntaxin13 (Prekeris *et al.*, 1998), is localized to endosomal fractions but absent from the P3 fraction. Thus, a significant fraction of the cellular pools of GLUT4, TfR, and IRAP are localized at steady state to small vesicles that contain Rab4 but lack other many other markers of early endosomes.

Discrete Populations of Small Vesicles Containing either GLUT4 or TfR Are Endocytic in Origin

To obtain evidence that the small vesicles in our preparation are derived along the endocytic pathway, we sought to label the vesicles by uptake of radiolabeled ligands. Cells were incubated with either radiolabeled transferrin or anti-myc monoclonal antibodies (9E10) at 0, 15, or 37°C. After the cells were washed to remove nonspecific label, the cells were homogenized, and the homogenate was subjected to velocity gradient centrifugation. Figure 2, A and B, shows the distribution of internalized ligands after internalization at different temperatures. At 37°C, both radiolabeled 9E10 (Figure 2A) and transferrin (Figure 2B) accumulate within slowly sedimenting vesicles. The ligands also cosediment with larger membranes at the bottom of the gradient, consistent with the labeling of endosomes and the plasma membrane. The distribution mirrors that observed at steady state (Figure 1). Soluble ligand is also seen at the top of the gradient. At 0 or 15°C, the internalized ligands cosediment to a similar degree with the larger membranes (endosomes or plasma membranes) but do not label the small vesicles, consistent with earlier observations (Wei *et al.*, 1998). Similarly, pulse-chase experiments show that when cells are incubated with radiolabeled ligands at 15°C to selectively label endosomes, and subsequently warmed to 37°C, labeling of small vesicles is also observed (Lim, Bonzelius, Low, Wille, Weimbs, and Herman, unpublished observations).

It is not clear from the above data whether surface-labeled TfR and GLUT4myc are targeted to one class of small vesicles or to discrete populations of ESVs that have a similar size. To address this issue, we utilized two experimental

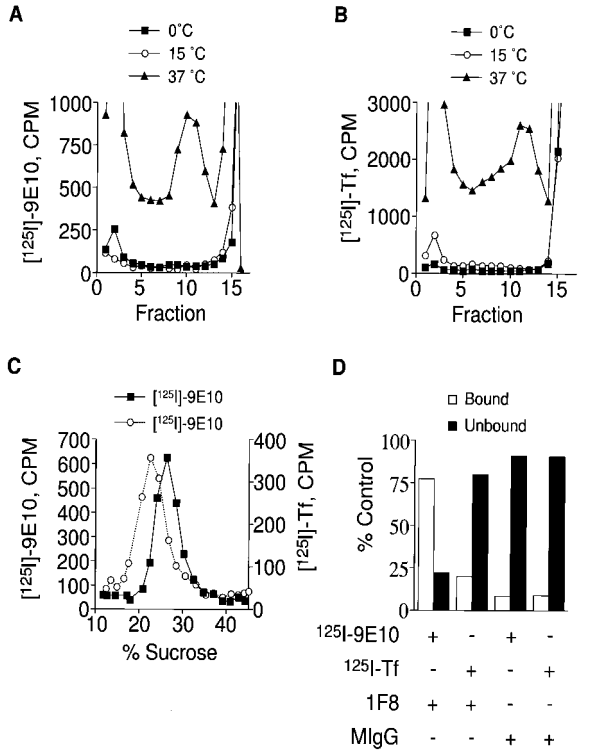

Figure 2. Labeling of ESVs by internalization of radiolabeled ligands. (A and B) Velocity sedimentation of homogenates. CHO/GLUT4myc cells were incubated with 5 μg/ml ^{125}I-9E10 (A) or ^{125}I-Tf (B) for 30 min at 37°C, 80 min at 15°C, or 2 h at 0°C and fractionated as described for Figure 1. Note targeting of the radiolabeled ligands to similar sized ESVs as those seen in Figure 1. (C) Separation of ESVs by equilibrium density centrifugation. Peak fractions from the glycerol gradients containing labeled ESVs were layered onto 10–45% sucrose gradients and centrifuged at 183,000 × *g* for 18 h. Note the different buoyant densities for ESVs containing transferrin (~22% sucrose) compared with ESVs containing 9E10 (~27% sucrose). (D) Immunoisolation of labeled ESVs. Radiolabeled homogenates were centrifuged at 27,000 × *g* for 30 min. The supernatant, enriched in ESVs, was incubated with anti-GLUT4 tail antibody (1F8) or mouse IgG overnight at 4°C and then centrifuged on glycerol gradients as above. Peak fractions containing the ESVs were incubated with protein G-Sepharose beads overnight at 4°C. The amount of each ligand bound to the beads was compared with the amount of ligand left behind in the unbound supernatant. Note the targeting of each ligand to discrete types of small vesicles. + denotes presence in assay; − denotes absence.

approaches, equilibrium density centrifugation and vesicle immunoisolation. In the first set of experiments, peak fractions from the glycerol gradients containing labeled ESVs (Figure 2, A and B) were layered onto sucrose gradients and centrifuged for 18 h at 183,000 × *g*. As shown in Figure 2C, ESVs containing radiolabeled transferrin have a different buoyant density (~22% sucrose) than ESVs containing radiolabeled 9E10 (~27% sucrose). In the second set of experiments, labeled homogenates were incubated with a monoclonal antibody recognizing the GLUT4 cytoplasmic tail (1F8) (James *et al.*, 1988) or with IgG before sedimentation on glycerol gradients. The peak fractions containing the labeled ESVs were then incubated with protein-G-Sepharose beads. Under conditions in which 1F8 specifically immunoadsorbs 50% of the ESVs labeled with radioiodinated 9E10, no specific adsorption above background levels is observed for ESVs labeled with radioiodinated transferrin (Figure 2D). The reciprocal experiments using antibodies against the TfR cytoplasmic tail (H68.4) (White *et al.*, 1992) were not successful, because the antibody did not appear to recognize native protein. These experiments suggest that ESVs containing GLUT4myc contain little or no transferrin. Thus, although ESVs containing transferrin and GLUT4myc have a similar size, they are distinct from one another as evidenced by different buoyant densities and discrete cargo compositions.

ESV Formation from Endosomes Can Be Reconstituted in a Cell-Free Assay

To provide direct evidence of the endosomal origin of ESVs and to gain access to the molecular components involved in the sorting of membrane proteins to ESVs and ESV formation, we established an in vitro assay that reconstitutes the formation of ESVs from endosomal membranes. A schematic of the assay is outlined in Figure 3. The assay is based on the fact that at 15°C ligands binding to the TfR or to GLUT4myc are internalized into endosomes but do not reach small vesicles (Wei *et al.*, 1998; Figure 2, A and B). Because the donor membranes can be selectively labeled, a relatively crude mixture of membranes can be utilized as starting material, bypassing the need to purify endosomes away from other organelles with similar physical characteristics. Crude membranes (containing the labeled endosomes) are pelleted and washed with urea-containing buffer to strip off peripheral membrane proteins associated with the cytosolic face of the membranes. The stripped membranes are pelleted and resuspended in Bud buffer (Clift-O'Grady *et al.*, 1998) (which approximates the electrolyte content of cytosol) with added cytosol and an ATP-regenerating system and warmed to 37°C. The entire reaction mixture is then layered onto a glycerol gradient and analyzed by velocity sedimentation. ESV formation is assayed by the appearance of radiolabeled ligand at the characteristic position in the middle of the gradients.

Figure 4, A and B, shows the product from a typical in vitro reaction using membranes selectively labeled at 15°C with either ^{125}I-9E10 or ^{125}I-transferrin, respectively. In the presence of 2 mg/ml rat brain cytosol, both ligands appear in vesicles that sediment at a similar position as those identified in intact cells. The efficiency of the assay was such that ~10–30% of the cell-associated radioactivity appeared in the de novo vesicles (Lim, Bonzelius, Low, Wille, Weimbs, and Herman, unpublished observations). In the absence of cytosol, there is some background budding that is probably a result of incomplete stripping of the endosomal membranes. When endosomal membranes are treated with milder buffers, including bud buffer or Tris-containing buffers, budding occurs even in the absence of cytosol (Lim, Bonzelius, Low, Wille, Weimbs, and Herman, unpublished observations). To verify that some of the de novo ESVs are not arising from labeled plasma membranes, we performed cell-free assays using membranes that were labeled at 0°C (Figure 4, C and D). Cells were incubated on ice for 2 h with either ^{125}I-transferrin or ^{125}I-9E10. A similar degree of cell-associated radioactivity is achieved as in the experiments conducted at 15°C. The cells were then processed in an identical manner

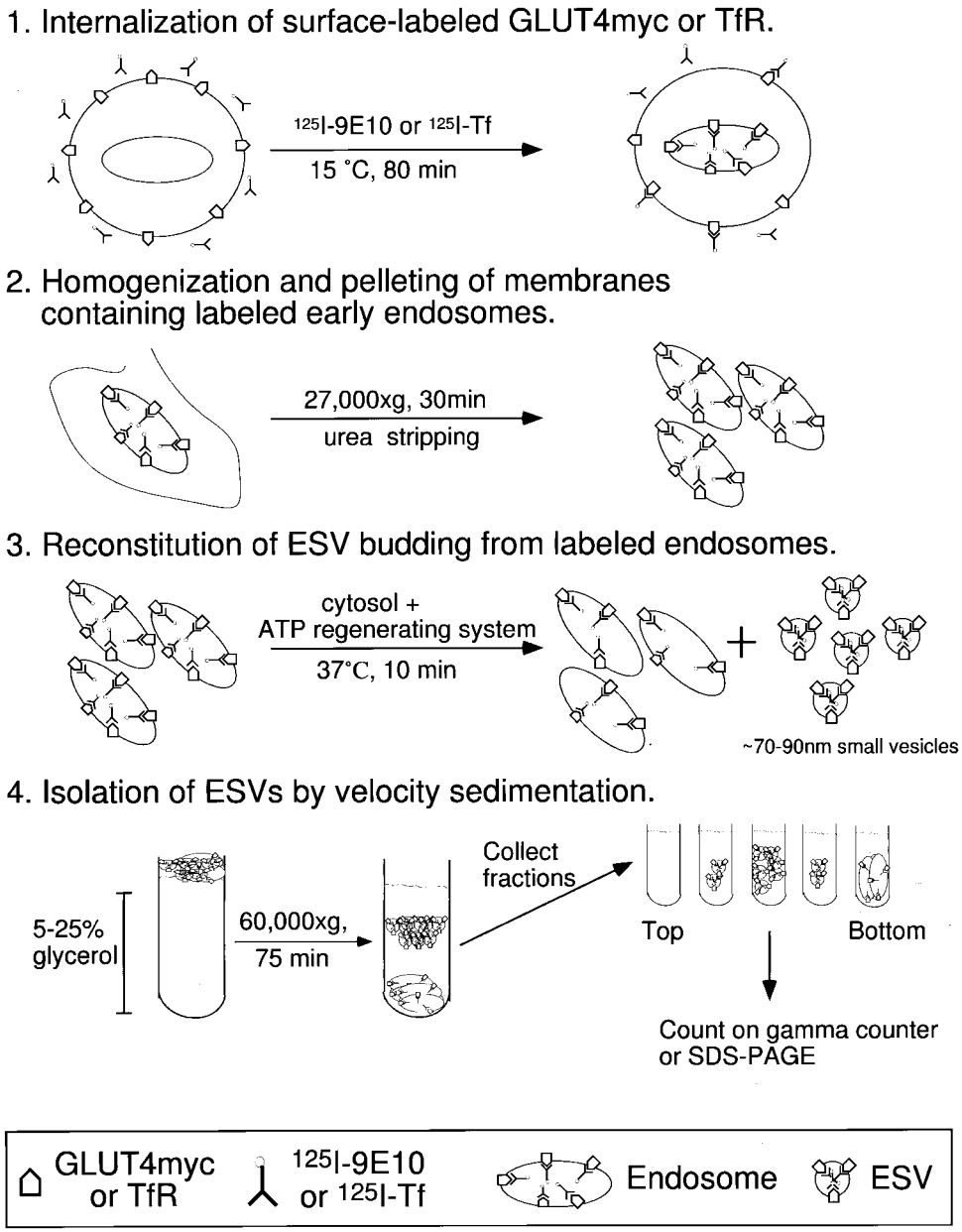

Figure 3. A cell-free assay for ESV formation from endosomes. (1) CHO/G4myc cells are incubated with ^{125}I-9E10 or ^{125}I-Tf for 80 min at 15°C to label early endosomes. (2) Cells are homogenized and centrifuged to pellet the labeled endosomes. Peripheral membrane proteins are removed from endosomes by treatment with buffer containing 2.5 M urea. The membranes are subsequently washed with Bud buffer. (3) Labeled membranes are incubated with cytosol in the presence of an ATP-regenerating system at 37°C, which, gives rise to ~70- to 90-nm small vesicles. (4) The reaction mixture is fractionated on glycerol gradients as described above. Gradient fractions are collected from the top and counted on a gamma counter or analyzed by SDS-PAGE and Western blot.

as the experiments shown in Figure 4, A and B. Unlike those experiments, neither ligand appears in de novo ESVs. These results indicate that the ESVs we observe in the cell-free assay after labeling membranes at 15°C arise from endosomal membranes and not labeled plasma membranes.

We also compared the efficiency of in vitro ESV formation from membranes enriched in plasma membranes with membranes enriched in endosomes (Figure 4E). To enrich the starting material for endosomal membranes, differential centrifugation was used. A 500 × *g* pellet (P1) contains 90% of the plasma membrane (as detected by the distribution of 0°C-labeled membranes) and some of the endosomal membranes. The supernatant left behind after a 500 × *g* spin was subjected to centrifugation at 27,000 × *g* to generate a pellet (P2) that is enriched in endosomal membranes. The efficiency of ESV production from the P2 was higher than that for the P1 for both TfR and GLUT4. These results are consistent with those that would be expected if the donor for the ESVs are endosomes rather than the plasma membrane.

Characterization of the Cell-Free Assay of ESV Formation

The cell-free assay of ESV formation was characterized. Figure 5A indicates the degree of ESV formation observed from membranes incubated with different concentrations of rat brain cytosol. The efficiency of ESV formation containing either radiolabeled transferrin or 9E10 increased with higher

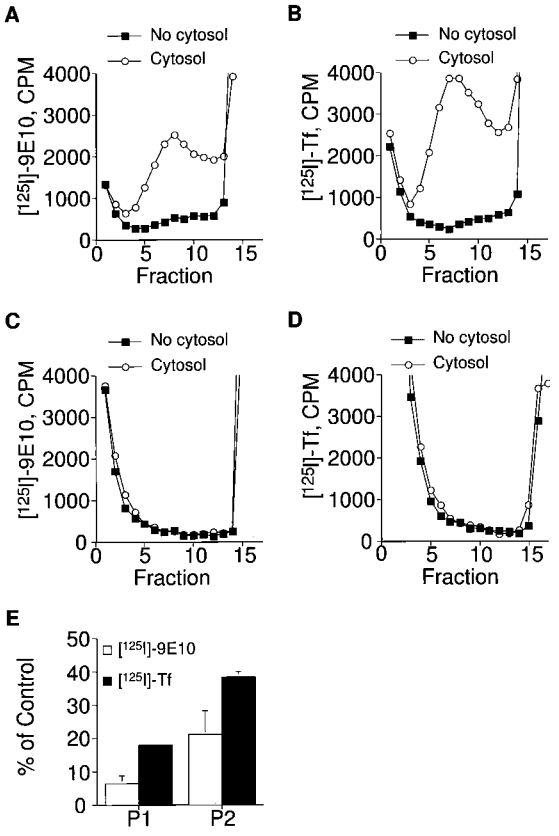

Figure 4. ESV formation can be reconstituted in a cell-free assay. (A and B) Cytosol dependence of ESV formation in vitro. CHO/GLUT4myc cells were incubated with either ^{125}I-9E10 (A) or ^{125}I-Tf (B), respectively, for 80 min at 15°C. Labeled crude membranes (1 mg/ml) were incubated for 10 min at 37°C with or without 2 mg/ml rat brain cytosol in the presence of an ATP-regenerating system. The entire reaction mixture was fractionated on glycerol gradients as described above. (C and D) Absence of detectable ESVs after in vitro budding from membranes labeled by incubation with ^{125}I-9E10 (C) or ^{125}I-Tf (D) for 2 h at 0°C. (E) Efficiency of ESV formation increases using donor membranes enriched in endosomal membranes. The formation of ESVs from different preparations of donor membranes was compared. P1, a pellet centrifuged at 500 × *g* (enriched in plasma membranes); P2, a pellet from the supernatant obtained after a 500 × *g* spin centrifuged at 27,000 × *g* (enriched in endosomal membranes). Values shown indicate the amount of specific radioactivity associated with de novo ESVs assayed on glycerol gradients normalized relative to the amount of specific radioactivity associated with the starting material in each reaction. The total amount of radioactivity recovered was the same for plus- and minus-cytosol conditions.

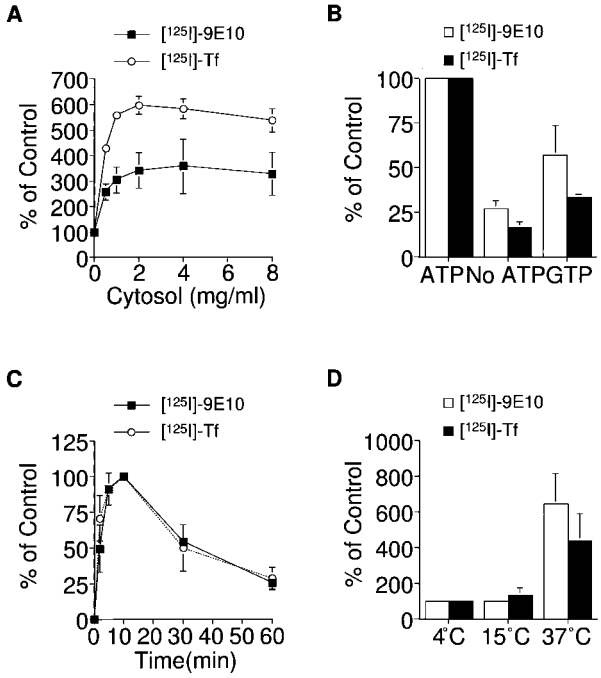

Figure 5. Characterization of the cell-free assay for ESV formation. (A) Cytosol concentration dependence of ESV biogenesis. Membranes (1 mg/ml) labeled with either ^{125}I-9E10 or ^{125}I-Tf were incubated with varying concentrations of rat brain cytosol in the presence of an ATP-regenerating system. Values are normalized relative to the minus-cytosol control. (B) Nucleotide dependence of ESV biogenesis. Budding from labeled membranes was carried out in the presence of cytosol with ATP, GTP, or no added nucleotide. Values were normalized relative to the amount of budding observed in the presence of 1 mM ATP. (C) Time course of ESV budding from labeled membranes at 37°C. Values were normalized relative to the maximal amount of ESV formation observed at 10 min. (D) Temperature dependence of ESV biogenesis. Budding from labeled membranes at either 0, 15, or 37°C. Values were normalized relative to the amount of budding observed at 0°C. The amount of specific radioactivity associated with de novo ESVs on glycerol gradients was determined for each reaction condition.

cytosol concentrations up to 1 mg/ml rat brain cytosol. Beyond 2 mg/ml cytosol, additional increases in the levels of ESV formation were not observed. A larger increase in cytosol-dependent budding was observed for ESVs containing transferrin (sixfold) than for ESVs containing 9E10 (3.5-fold). Similar results were observed when cytosol obtained from other tissues (liver, adipose, skeletal and cardiac muscle) was substituted for brain cytosol in the in vitro reaction (Lim, Bonzelius, Low, Wille, Weimbs, and Herman, unpublished observations). Thus, the budding of ESVs from endosomes seems to have different cytosol requirements than the budding of synaptic like microvesicles (Desnos *et al.*, 1995).

ATP is also required (Figure 5B). When ATP is excluded from the reaction mixture, the levels of ESV formation observed approximate that of the background levels observed in the minus-cytosol controls described above (Figure 4, A and B). Added GTP is able to provide a modest stimulation in ESV formation. However, this may be due to the conversion of GTP to ATP or the presence of contaminant ATP in the preparation and may not reflect a true requirement for GTP.

A time course for ESV formation containing either ligand showed unusual kinetics (Figure 5C). Membranes containing internalized ^{125}I-transferrin or ^{125}I-9E10 were incubated with cytosol and an ATP-regenerating system at 37°C for various periods of time. The maximum extent of ESV formation occurs within 10 min. The maximal rate of ESV formation is observed within the first 5 min of the reaction. Beyond 10 min of incubation at 37°C, there is a significant

diminution in the degree of ESV formation observed. Addition of *n*-ethyl maleimide (NEM) to the reaction mixture prevents this decline (Lim, Bonzelius, Low, Wille, Weimbs, and Herman, unpublished observations). We speculate that the decrease in ESV formation observed after 10 min may in part be due to fusion of the budded ESVs with each other or with other membranes (endosomes, plasma membrane) still present in the reaction mixture. According to this explanation, at times earlier than 10 min, the rate of vesicle biogenesis would exceed the rate of vesicle fusion.

The temperature dependence of the reaction was measured (Figure 5D). Consistent with the results observed in intact cells (Figure 1B), increases in ESV formation above background levels were not observed at 0 or 15°C.

ESV Formation from Endosomes Is Mediated by a BFA-insensitive GTPase(s) and Inhibited by Neomycin

GTP-binding proteins mediate most vesicular transport processes. These have been shown to be involved in the recruitment of coat proteins (e.g., ARF1, Sar1) to a donor organelle as well as vesiculation of the nascent bud (e.g., dynamin; Holroyd *et al.*, 1999; Springer *et al.*, 1999; Mellman and Warren, 2000). We sought to determine whether ESV formation was sensitive to the addition of nonhydrolyzable analogues of GTP. Addition of nonhydrolyzable GTP analogues, GTPγS or GMP-PNP resulted in the reduction of ESV formation from donor membranes to or below background levels (Figure 6A). Although a GTPase appears to be involved in ESV formation, its action was not sensitive to the addition of the fungal metabolite, BFA (Figure 6B). Despite the addition of up to 400 μg/ml BFA, the levels of de novo ESVs did not appreciably decrease. Furthermore, when BFA was added simultaneously with the internalization of radiolabeled ligands at 37°C in intact cells, no reduction in the delivery of the ligands to ESVs was observed (Lim, Bonzelius, Low, Wille, Weimbs, and Herman, unpublished observations). These results suggest that the ARF1 GTPase-activating protein in this cell line is insensitive to inhibition by BFA or, alternatively, that ARF1 is not involved in ESV formation. Consistent with the latter possibility, addition of dominant active (Q71L) or dominant negative (T31N) mutant forms of recombinant ARF1 (Randazzo *et al.*, 1992) to the reaction mixtures did not significantly alter levels of ESV production (Lim, Bonzelius, Low, Wille, Weimbs, and Herman, unpublished observations). Thus, ESV formation appears to be mediated by one or more BFA-insensitive GTPases.

Phospholipase D (PLD) has been postulated to be a downstream effector of ARF (Kahn *et al.*, 1993; Cockcroft, 1996) mediating budding of Golgi vesicles (Ktistakis *et al.*, 1996), adaptor recruitment to endosomes (West *et al.*, 1997), and endosome-endosome fusion (Jones and Wessling-Resnick, 1998). PLD has been proposed to facilitate coat recruitment to donor membranes by increasing the local production of phosphatidic acid and phosphatidylinositol 4,5-biphosphate (PIP2; Ktistakis *et al.*, 1996). To investigate the potential role of PLD in ESV formation, we assayed the effects of neomycin on ESV formation. Neomycin, an aminoglycoside, has been shown to inhibit PIP2-dependent PLD indirectly by binding PIP2 (Liscovitch *et al.*, 1994; West *et al.*, 1997; Jones and Wessling-Resnick, 1998). When varying concentrations of neomycin are added to labeled endosomal membranes, we observe a dose-dependent inhibition of ESV formation (Figure 6C). Poly-L-aspartic acid, which binds to PIP2-containing membranes and displaces aminoglycosides (Kishore *et al.*, 1990), has been shown to reverse the inhibition of PLD by neomycin (Jones and Wessling-Resnick, 1998). Including poly-L-aspartic acid in the reaction mixture (Figure 6D) prevents inhibition of ESV formation by neomycin. Thus, the inhibitory action of neomycin appears to be specific to phospholipid binding and not due to detergent-like effects on the endosomal membranes.

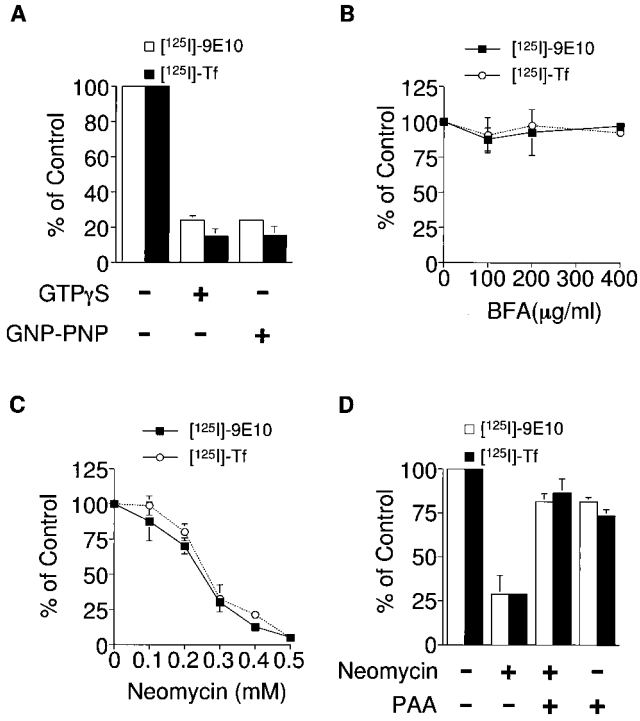

Figure 6. Inhibition of ESV formation by nonhydrolyzable analogues of GTP and neomycin. (A) ESV formation in vitro was assayed in the presence of nonhydrolyzable GTP analogues, 200 μM GTPγS or 200 μM GMP-PNP plus cytosol and an ATP-regenerating system. (B) ESV formation in vitro was assayed in the presence of varying concentrations of BFA. (C) ESV formation in vitro was assayed in the presence of varying concentrations of neomycin. Donor membranes and cytosol were preincubated with neomycin for 15 min at 0°C. (D) Inhibition of ESV formation by neomycin is prevented by the addition of poly-L-aspartic acid (PAA). Neomycin (0.3 mM) and/or poly-L-aspartic acid (0.03 mM) were preincubated with membranes and cytosol as above.

ESVs Generated In Vitro Resemble Those Isolated from Intact Cells

To ensure that the cell-free assay faithfully reproduces the vesicle formation that occurs in intact cells, we compared the appearance and composition of ESVs formed in the cell-free assay with those isolated from intact cells. Figure 7 shows the results from electron microscopy experiments. First, ESVs were isolated from intact cells by collecting the peak

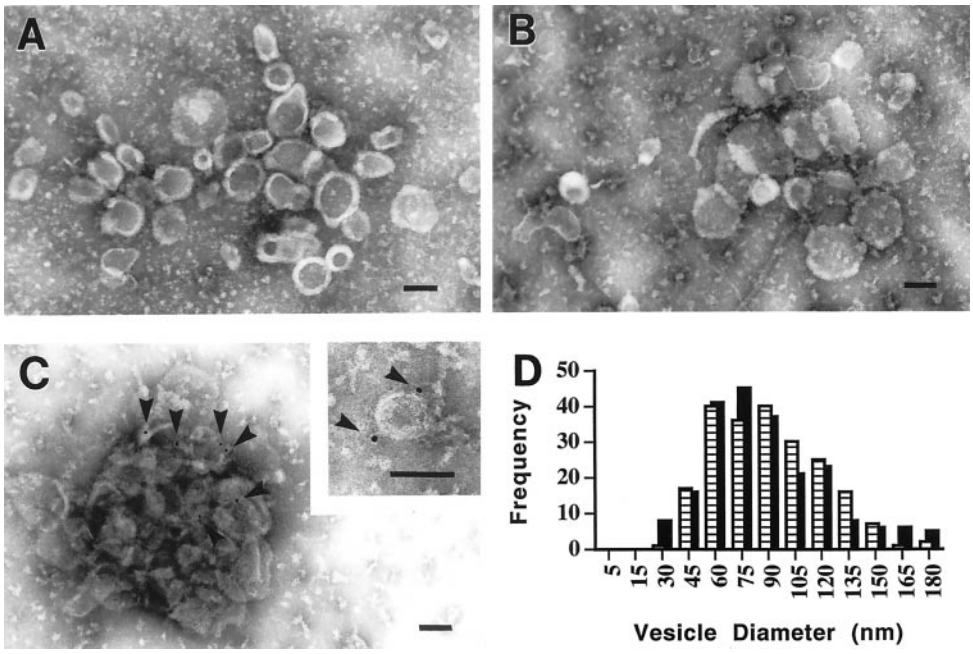

Figure 7. Negative stain electron micrographs of ESVs isolated from intact cells and generated in vitro. (A) ESVs isolated from intact CHO/GLUT4myc cells. (B) Vesicles generated in vitro from CHO/GLUT4myc cell membranes. (C) In vitro generated vesicles immunogold labeled with anti-GLUT4 polyclonal antibody R820. The inset shows a magnified image of a single in vitro generated vesicle carrying two gold particles (arrowheads). (D) Histogram showing the size distributions of in vivo (hatched bars) and in vitro (solid bars) generated vesicles. Both types of vesicles show a similar size distribution with a median external diameter of ~70–90 nm. Negative stain, 2% ammonium molybdate. Bars, 100 nm.

fractions from glycerol gradients after velocity sedimentation. The ESVs were adsorbed onto grids, negatively stained with ammonium molybdate, and visualized with an electron microscope. Similar samples were prepared by isolating de novo ESVs after budding from labeled endosomal membranes. The clusters of vesicles shown in Figure 7, A and B, demonstrate typical membrane stain exclusion and are essentially indistinguishable in appearance from one another. The external diameter of individual vesicles was measured and the size histogram of ESVs isolated from intact cells compared with that of ESVs generated in the cell-free assay (Figure 7D). The size distribution of ESVs was very similar because both types of preparations of vesicles showed a median diameter of ~70–90 nm.

The samples visualized in Figure 7B did not appear to contain any pre-existing ESVs that were present in the preparation before budding at 37°C. When the in vitro reactions were carried out in the absence of cytosol or at 0°C, no ESVs could be detected in samples prepared from the gradient fractions corresponding to those obtained above. The starting material contained large, tubular structures without any apparent free or attached small vesicles (Lim, Bonzelius, Low, Wille, Weimbs, and Herman, unpublished observations). ESVs isolated under both conditions showed a similar pattern of immunogold labeling when the ESVs were incubated with an anti-GLUT4 cytoplasmic tail polyclonal antibody (Figure 7C).

We next assayed the composition of de novo ESVs and those isolated from intact cells (Figure 8). In vivo and in vitro generated ESVs were isolated on glycerol gradients. Peak fractions containing the ESVs were incubated with protein G-Sepharose beads coupled to the anti-GLUT4 cytoplasmic tail monoclonal antibody, 1F8, or to IgG-coupled beads. SDS-PAGE and Western blot were used to analyze the starting material (SM) containing ESVs isolated from the gradients or ESVs associated with the 1F8-beads (1F8) or IgG-beads (IgG). The 1F8-coupled beads are able to adsorb most of the GLUT4 associated with in vivo as well as in vitro generated ESVs. The 1F8-coupled beads also adsorb all of the IRAP associated with ESVs. In contrast, almost none of the TfR is adsorbed, consistent with the results shown in Figure 2D. The same results are observed whether or not the ESVs are labeled with internalized 9E10 before immunoisolation. The observation of different vesicle populations therefore cannot be explained by cross-linking of a subset of vesicles by the 9E10 antibody. Thus, at least two classes of ESVs are identified; those enriched in GLUT4 and IRAP and those that contain TfR. Segregation into these discrete classes of ESVs is preserved in the cell-free assay.

ESVs adsorbed by the 1F8-beads also contain the endosomal v-SNARE, cellubrevin (vesicle-associated membrane protein 3; McMahon *et al.*, 1993; Daro *et al.*, 1996). Because most of the cellubrevin is adsorbed under these conditions, it is unclear which v-SNARE is associated with the ESVs enriched in TfR. We were not able to detect any vesicle-associated membrane protein 2 or endobrevin associated with either class of small vesicles (Lim, Bonzelius, Low, Wille, Weimbs, and Herman, unpublished observations). However, the amount of immunodetectable signal was very low, even that obtained from crude membranes. Consistent with the results presented above, Rab11, EEA1, and syntaxin 13 were not detected in either in vivo or in vitro generated ESVs (Lim, Bonzelius, Low, Wille, Weimbs, and Herman, unpublished observations). Thus, the composition of ESVs generated in vitro appears very similar to those isolated from intact cells.

Inhibition of the Targeting of GLUT4 to ESVs

The sorting of transmembrane cargo into vesicles budding from donor organelles appears to involve the interaction of the cytoplasmic tails of the membrane proteins with cytoso-

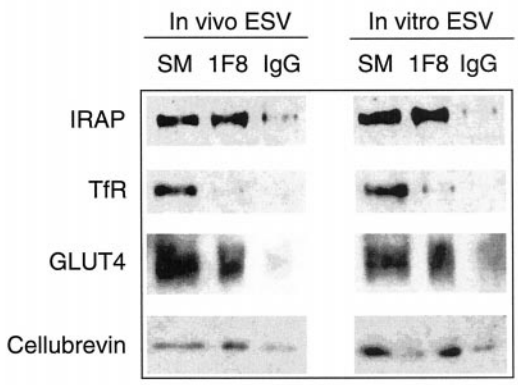

Figure 8. Western blot analysis of in vivo and in vitro generated ESVs after immunoisolation. ESVs labeled in intact cells (in vivo) or in vitro generated ESVs were isolated from glycerol gradients and incubated overnight at 4°C with protein G-Sepharose beads cross-linked to either 1F8 or mouse IgG. The starting material (SM; the peak glycerol gradient fractions containing the ESVs) and the 1F8-bead (1F8) or IgG-bead (IgG) eluates were subjected to SDS-PAGE and Western blot analysis. Note that under both conditions TfR is largely excluded from ESVs enriched in GLUT4 and IRAP. The v-SNARE cellubrevin is localized to the ESVs.

lic coat proteins (Kirchhausen *et al.*, 1997). We sought to more directly determine the selectivity of cargo recruitment into the newly budded ESV. Monoclonal antibodies are available that will bind to and interact with the cytoplasmic tail of GLUT4 in its native state (James *et al.*, 1988). If inclusion of GLUT4 into the ESVs occurs by selective recruitment, then it may be possible to hinder the inclusion of GLUT4 into de novo ESVs by sterically interfering with the interaction of the GLUT4 tail with cytosolic proteins using those antibodies. If, on the other hand, the targeting of GLUT4 into ESVs is passive, then the inclusion of GLUT4 into ESVs should be unaffected by agents that interact with the GLUT4 tail.

Endosomal membranes labeled by internalization of radiolabeled transferrin or 9E10 at 15°C were preincubated with the anti-GLUT4 tail antibody, 1F8, before the addition of cytosol and an ATP-regenerating system. Incubation of the endosomal membranes with 1F8 results in an ~40% decrease in the delivery of radiolabeled anti-myc monoclonal antibodies to ESVs but has very little effect on the targeting of transferrin to ESVs (Figure 9A). Addition of mouse IgG has almost no effect. When the 1F8 antibody is preincubated with a GST-fusion protein containing the GLUT4 carboxy terminus (GST-GLUT4tail), the inhibitory effect of the antibody is no longer observed. However, the GST-GLUT4tail alone is without effect. We hypothesize that the affinity of the fusion protein for the cytosolic sorting machinery is too low to competitively inhibit association of the native, full-length GLUT4 with the cytosolic proteins.

The reaction products were also analyzed by SDS-PAGE and Western blot. The amount of GLUT4, TfR, and IRAP localized to ESVs was compared after preincubation with either the 1F8 antibody or an IgG control. As shown in Figure 9B, the amount of GLUT4 localized to de novo ESVs is reduced by ~50% after incubation of the donor endosomal membranes with the 1F8 antibody as compared with the IgG control. However, formation of the class of ESVs that normally contain GLUT4, as assayed by the presence of IRAP, was unperturbed. The amounts of IRAP associated with the ESVs were the same or higher than the IgG control. This argues against an artifact whereby addition of the 1F8 to the reaction mixture cross-links a subset of the vesicles, making them heavier than usual. The amounts of TfR associated with the other class of ESVs were also the same or higher than the IgG control, consistent with the results from Figure 9A. Taken together, these results suggest that inclusion of the 1F8 antibody into the cell-free reaction disrupts the association of the GLUT4 carboxy terminus with cytosolic sorting machinery. Thus, the entry of GLUT4 into ESVs can be selectively inhibited without interfering with the targeting of other cargo proteins to the ESVs.

DISCUSSION

According to vesicular transport models, trafficking of membrane proteins is mediated by the formation of transport vesicles that capture cargo proteins from a donor organelle and carry the cargo to an acceptor organelle where they fuse (Holroyd *et al.*, 1999; Springer *et al.*, 1999; Mellman and Warren, 2000). However, it has been difficult to validate this model with respect to the transport of recycling plasma membrane proteins from early endosomes. In particular, transport vesicles carrying recycling plasma membrane proteins have not yet been identified. Here, we report the identification of at least two classes of small vesicles of endosomal origin, the ESVs, which are enriched in either the TfR or GLUT4 and IRAP and which have unique buoyant densities. To validate the endosomal origin of the ESVs, we also describe the efficient cell-free reconstitution of ATP-, temperature-, and cytosol-dependent budding of these ESVs from labeled endosomal membranes. ESVs do not form from plasma membranes labeled at 0°C. Although we do not yet know the ultimate fate of the ESVs, a model describing the potential role of ESVs in the trafficking of recycling plasma membrane proteins is shown in Figure 10.

Surprisingly, we found that a significant fraction of the total pools of GLUT4, TfR, and IRAP are localized to ESVs at steady state (Figure 1A). Although GLUT4 has been shown to localize to small vesicles that exclude TfR in fat and muscle cells (Livingstone *et al.*, 1996; Martin *et al.*, 1996; Malide *et al.*, 1997; El-Jack *et al.*, 1999; Lee *et al.*, 1999; Hashiramoto and James, 2000), the abundance of ESVs containing GLUT4 in other cell types has been underestimated. The targeting of TfR to other classes of small vesicles has also not been previously reported. There are a number of possible explanations for these discrepancies. First, the ESVs may have been lost during homogenization because 50% of the small vesicles escape from cells during removal of the cells from dishes (Müller, unpublished data). Because less TfR than GLUT4 is localized to ESVs, the loss of small vesicles was such that the presence of TfR within ESVs was not detected in our earlier work (Herman *et al.*, 1994; Wei *et al.*, 1998). Second, the ESVs may be difficult to distinguish from endosomes by immunofluorescence techniques because

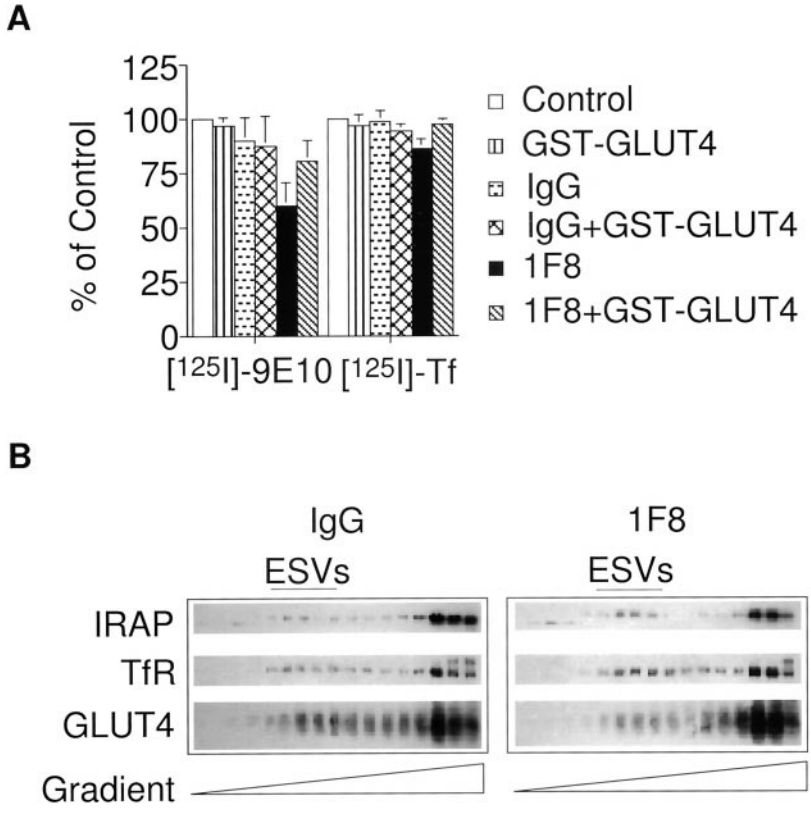

Figure 9. Anti-GLUT4 tail antibodies interfere with the targeting of GLUT4 to de novo ESVs. (A) Targeting of radiolabeled ligands to ESVs. Endosomal membranes labeled with either ^{125}I-9E10 or ^{125}I-Tf were preincubated with either 100 μg/ml monoclonal anti-GLUT4 antibody 1F8, 1F8 plus 4 mg/ml GST-GLUT4 tail fusion protein, GST-GLUT4 tail fusion protein alone, or 100 μg/ml mouse IgG for 30 min at 4°C. Budding was measured by the addition of cytosol and an ATP-regenerating system and warming to 37°C for 10 min. The reaction mixtures were analyzed by velocity sedimentation as described above. Gradient fractions were counted on a gamma counter. (B) Analysis of targeting to ESVs by Western blot. Gradient fractions were precipitated with 6% trichloroacetic acid, subjected to SDS-PAGE, and analyzed by Western blot. ESV budding after inclusion of the 1F8 antibody in the reaction mixture was compared with IgG controls. Note the selective inhibition of targeting of GLUT4 but not IRAP or the TfR to the newly formed ESVs.

light microscopic techniques do not resolve vesicles of this size. Third, because of their small size, the abundance of ESVs may be underestimated by electron microscopy of thin sections. Moreover, it is difficult to distinguish small vesicles from tubules that have been transverse sectioned. Electron microscopy of thin sections in fat and muscle cells does reveal that GLUT4 localizes to tubulovesicular structures (Slot *et al.*, 1991a,b; Smith *et al.*, 1991; Rodnick *et al.*, 1992). Using a novel electron microscopy technique, abundant similarly sized small vesicles containing GLUT4 can be more clearly identified in unsectioned cells (Ramm *et al.*, 2000).

Although it is possible that fragmentation of endosomes could give rise to small vesicles, this is an unlikely explanation of our findings. First, ESVs of similar size, appearance, and composition are observed from intact cells using a variety of homogenization techniques as well as the product of cell-free assays where no shearing forces are applied. Second, in the absence of ATP or cytosol, no ESV formation is observed in vitro. Third, the selective inclusion of Rab4 and cellubrevin and exclusion of other early endosomal markers such as Rab11, EEA1, and syntaxin13 from ESVs argues against a fragmentation mechanism. Fourth, the selective disruption of GLUT4 targeting to the ESVs using antibodies against the GLUT4 tail also argues against such a mechanism. Finally, although BFA causes increased endosomal tubulation with transferrin localizing to an extensive tubular network (Lippincott-Schwartz *et al.*, 1991; Tooze and Hollinshead, 1992; Daro *et al.*, 1996), we did not see an increase in the localization of transferrin to ESVs. If ESVs were forming as a result of fragmentation of tubules, we would expect to observe an increase in the amount of ESVs after BFA treatment.

What is the function of the ESVs? Given their size, it is unlikely that ESVs can be considered sorting organelles. If they are true carrier vesicles, they should fuse with an acceptor membrane. Current evidence, albeit preliminary, supports a carrier role. The time course of ESV formation from endosomes in the cell-free assay implies that after 10 min the ESVs disappear, presumably by undergoing fusion with other membranes in the preparation (Figure 5C). This idea is reinforced by the observation that NEM can prevent this decline. In intact cells, under conditions in which targeting to ESVs is inhibited, ESVs labeled with internalized GLUT4myc disappear with kinetics that mirror the kinetics of the surface appearance of the transporter (Wei *et al.*, 1998). In preliminary experiments, we have also been able to reconstitute the NEM-sensitive fusion of ESVs with other membranes, but so far we have been unable to discern whether the acceptor membranes are the plasma membrane or another endosomal compartment (Lim and Herman, unpublished data).

The ESVs do not appear to be identical to pericentriolar recycling endosomes enriched in Rabs 4 and 11 (Sheff *et al.*, 1999; Sönnichsen *et al.*, 2000). At steady state in CHO cells, GLUT4, TfR, and IRAP do accumulate in pericentriolar structures as visualized by immunofluorescence microscopy (Yamashiro *et al.*, 1984; Johnson *et al.*, 1998). However, in addition to the fact that ESVs lack Rab11, purification of the recycling endosomes on optiprep gradients followed by electron microscopy reveals structures that are two to three

times the size of ESVs observed here (Sheff *et al.*, 1999). We propose that ESVs serve as transport vesicles to carry recycling membrane proteins from early endosomes to either pericentriolar recycling endosomes or directly to the cell surface. Because GLUT4 and TfR label discrete structures at 15°C (Wei *et al.*, 1998), ESVs containing GLUT4 or IRAP may bud from different subdomains of the same endosome or physically separate endosomes than ESVs enriched in TfR.

The fact that the ESVs are so abundant raises the possibility that, in addition to serving a role as transport intermediates, they may be involved in the intracellular storage of the plasma membrane proteins, providing a reserve pool for modification of the cell surface. Alternatively, the flow of proteins through short-lived transport vesicles could be so great that the ESVs are easily detected at steady state. We find that GLUT4, TfR, and IRAP accumulate within ESVs to varying degrees. Differences in the abundance of ESVs may arise if the rates of ESV formation and fusion with acceptor membranes vary with different classes of ESVs and in different cell types, allowing for additional levels of regulation. In the case of the class of ESVs containing IRAP and GLUT4, our results are consistent with observations in fat and muscle cells showing differential targeting of the proteins to small vesicles (Aledo *et al.*, 1997; Martin *et al.*, 1997; Ross *et al.*, 1998). These differences may result in part from variation in the efficiency of sorting of each of the membrane proteins from endosomes to the ESVs. In insulin-responsive fat and muscle cells, we have observed that 90% of the cell-associated GLUT4 is localized to small vesicles at steady state (Kallay and Herman, unpublished data). The abundance of ESVs, even in CHO cells, is consistent with our earlier hypothesis (Herman *et al.*, 1994) that many cell types might use an ESV storage mechanism to allow rapid alteration of the composition of the plasma membrane.

The in vitro assay of ESV formation presented here provides a functional basis to study the molecular requirements of the targeting of recycling membrane proteins to ESVs from endosomes. The cell-free assay appears to faithfully reconstitute the targeting to ESVs that is observed in intact cells. ESVs isolated from intact cells have the same appearance and size by electron microscopy and the same biochemical composition as ESVs generated in vitro. The sorting of GLUT4 and TfR to separate compartments in vitro is also consistent with our earlier observations in intact cells (Wei *et al.*, 1998). We have only begun to understand the molecular events involved. Although a GTPase is involved, ESV formation is insensitive to BFA. Consistent with this observation is the fact that the recycling of transferrin is largely BFA resistant (Lippincott-Schwartz *et al.*, 1991) and transport of transferrin from Rab4/Rab5-positive early endosomes to Rab4/Rab11-recycling endosomes proceeds in the presence of BFA (Sönnichsen *et al.*, 2000). Although ESV formation is resistant to BFA, PIP2-sensitive PLD, a downstream effector of ARF, may be involved in this process, as evidenced by the inhibition of ESV biogenesis by neomycin. It is possible that ARFs mediate coat recruitment to early endosomes and ESV formation but that the ARF exchange factors localized to the early endosomes are resistant to BFA. Alternatively, other stimulators of PLD may be involved or the catalytic activity of PLD on endosomal membranes in CHO cells might be high enough to bypass a requirement for ARFs in coat recruitment. Because neomycin inhibits PLD indirectly by binding to PIP2, it is also possible that PIP2 plays a more direct role in coat recruitment, independently of PLD activity. Such a role for PIP2 has been suggested in the recruitment of coat proteins such as AP2 and accessory proteins such as dynamin to coated pits (Corvera *et al.*, 1999). Although we do not yet know which coat proteins are required for membrane protein targeting to ESVs and ESV formation, preliminary experiments indicate that in the presence of nonhydrolyzable analogues of GTP, subunits of clathrin, AP1, AP2, and dynamin are recruited from cytosol to immunoisolated ESVs (Lim, Bonzelius, Low, Wille, Weimbs, and Herman, unpub-

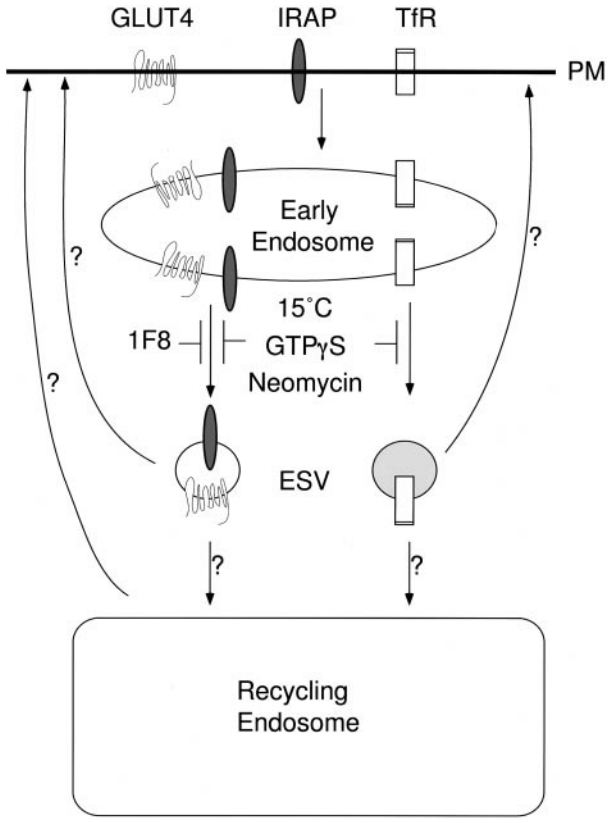

Figure 10. Model-discrete classes of ESVs store and carry recycling membrane cargo from early endosomes. TfR and GLUT4 are internalized from the cell surface into discrete domains of early/sorting endosomes (or to physically separate early endosomes). IRAP is internalized into the same domains occupied by GLUT4. GLUT4 and IRAP are targeted into one class of ESVs, whereas TfR is targeted to another population of discrete ESVs. Other classes of ESVs, not yet identified, may also exist. Transport from early endosomes to both classes of ESVs is inhibited at 15°C and is mediated by one or more BFA-insensitive GTPases and PIP2-dependent PLD or directly by PIP2. Because entry of GLUT4 into ESVs can be perturbed with anti-cytoplasmic tail antibodies, we propose that the entry of cargo into nascent ESVs is facilitated by an interaction of the cytoplasmic tails of the recycling plasma membrane (PM) proteins with cytosolic proteins. ESVs, containing Rab4 and the v-SNARE cellubrevin, may carry the recycling membrane proteins to pericentriolar recycling endosomes or directly to the cell surface. Because they are so abundant, the ESVs may also function as a storage depot, delivering the cargo to targets at variable rates.

lished observations). Validation of the putative role of these proteins awaits further experimentation.

The most important observation so far from the in vitro reconstitution assay is that the targeting of recycling membrane proteins to ESVs from endosomes appears to be selective. Inclusion of an antibody against the GLUT4 carboxy terminus is able to impede the incorporation of GLUT4 into newly formed ESVs without disrupting the delivery of IRAP to the same class of ESVs or TfR to the other class of ESVs (Figure 9). Although we cannot rule out retention of GLUT4 within endosomes as a result of cross-linking of GLUT4 molecules by the 1F8 antibody, we favor an explanation whereby the antibody sterically interferes with the interaction of the cytoplasmic domains of the transmembrane cargo with cytosolic proteins. These data argue against a mechanism whereby cargo proteins would be passively included in the budding ESVs or one in which ESVs form by random vesiculation of endosomal membranes. Our experiments also suggest that the inclusion of cargo into the nascent vesicles can be uncoupled from vesicle budding. This is in contrast to recent studies linking cargo selection to vesiculation (Salem *et al.*, 1998; Springer and Schekman, 1998; Haucke and De Camilli, 1999). Cytosolic proteins involved in the sorting of cargo proteins to ESVs might be useful targets for the development of therapeutic agents to modulate the trafficking of select plasma membrane proteins. For instance, in type 2 diabetes, there is diminished redistribution of GLUT4 to the cell surface in response to insulin, resulting in elevated blood sugar levels (Kahn, 1998). Inhibition of the sorting of GLUT4 to ESVs by interfering with these cytosolic proteins might redirect enough GLUT4 to the cell surface to correct the hyperglycemia. Studies will need to be performed in fat and muscle cells to determine wether similar mechanisms influence the sorting of GLUT4 in insulin-responsive cells.

ACKNOWLEDGMENTS

We thank Michael Bishop, Samuel Cushman, Reinhard Jahn, Susanna Keller, and Paul Pilch for generously providing antibodies. We are grateful to Yousuke Ebina for generously providing the CHO/G4myc cell line. We very much appreciate Victor Faundez, Regis Kelly, and Keith Mostov for providing critical input concerning the manuscript. We extend special thanks to Leslie Spector for outstanding administrative support. This work was supported by grants from the National Institutes of Health (grant DK02163) and the American Diabetes Association (to G.A.H.), the Korean Science and Engineering Foundation (to S.-N.L.), and the Deutsche Forschungsgemeinschaft (to F.B.; grant SFB 474, C6).

REFERENCES

Aledo, J.C., Lavoie, L., Volchuk, A., Keller, S.R., Klip, A., and Hundal, H.S. (1997). Identification and characterization of two distinct intracellular GLUT4 pools in rat skeletal muscle: evidence for an endosomal and an insulin-sensitive GLUT4 compartment. Biochem. J. *325*, 727–732.

Bonifacino, J.S., and Weissman, A.M. (1998). Ubiquitin and the control of protein fate in the secretory and endocytic pathways. Annu. Rev. Cell Dev. Biol. *14*, 19–57.

Bonzelius, F., Herman, G.A., Cardone, M.H., Mostov, K.E., and Kelly, R.B. (1994). The polymeric immunoglobulin receptor accumulates in specialized endosomes but not synaptic vesicles within the neurites of transfected neuroendocrine PC12 cells. J. Cell Biol. *127*, 1603–1616.

Chavrier, P., Parton, R.G., Hauri, H.P., Simons, K., and Zerial, M. (1990). Localization of low molecular weight GTP binding proteins to exocytic and endocytic compartments. Cell *62*, 317–329.

Clague, M.J. (1998). Molecular aspects of the endocytic pathway. Biochem. J. *336*, 271–282.

Clift-O'Grady, L., Desnos, C., Lichtenstein, Y., Faúndez, V., Horng, J.T., and Kelly, R.B. (1998). Reconstitution of synaptic vesicle biogenesis from PC12 cell membranes. Methods *16*, 150–159.

Cockcroft, S. (1996). ARF-regulated phospholipase D: a potential role in membrane traffic. Chem. Phys. Lipids *80*, 59–80.

Cormont, M., Bortoluzzi, M.N., Gautier, N., Mari, M., van Obberghen, E., and Le Marchand-Brustel, Y. (1996). Potential role of Rab4 in the regulation of subcellular localization of Glut4 in adipocytes. Mol. Cell. Biol. *16*, 6879–6886.

Corvera, S., D'Arrigo, A., and Stenmark, H. (1999). Phosphoinositides in membrane traffic. Curr. Opin. Cell Biol. *11*, 460–465.

Daro, E., van der Sluijs, P., Galli, T., and Mellman, I. (1996). Rab4 and cellubrevin define different early endosome populations on the pathway of transferrin receptor recycling. Proc. Natl. Acad. Sci. USA *93*, 9559–9564.

de Wit, H., Lichtenstein, Y., Geuze, H.J., Kelly, R.B., van der Sluijs, P., and Klumperman, J. (1999). Synaptic vesicles form by budding from tubular extensions of sorting endosomes in PC12 cells. Mol. Biol. Cell *10*, 4163–4176.

Desnos, C., Clift-O'Grady, L., and Kelly, R.B. (1995). Biogenesis of synaptic vesicles in vitro. J. Cell Biol. *130*, 1041–1049.

El-Jack, A.K., Kandror, K.V., and Pilch, P.F. (1999). The formation of an insulin-responsive vesicular cargo compartment is an early event in 3T3–L1 adipocyte differentiation. Mol. Biol. Cell *10*, 1581–1594.

Faúndez, V., Horng, J.T., and Kelly, R.B. (1997). ADP ribosylation factor 1 is required for synaptic vesicle budding in PC12 cells. J. Cell Biol. *138*, 505–515.

Faúndez, V., Horng, J.-T., and Kelly, R.B. (1998). A function for the AP3 coat complex in synaptic vesicle formation from endosomes. Cell *93*, 423–432.

Futter, C., Gibson, A., Allchin, E., Maxwell, S., Ruddock, I., Odorizzi, G., Domingo, D., Trowbridge, I., and Hopkins, C. (1998). In polarized MDCK cells basolateral vesicles arise from clathrin-gamma-adaptin-coated domains on endosomal tubules. J. Cell Biol. *141*, 611–623.

Grote, E., and Kelly, R.B. (1996). Endocytosis of VAMP is facilitated by a synaptic vesicle targeting signal. J. Cell Biol. *132*, 537–547.

Gruenberg, J., and Maxfield, F.R. (1995). Membrane transport in the endocytic pathway. Curr. Opin. Cell Biol. *7*, 552–563.

Hashiramoto, M., and James, D.E. (2000). Characterization of insulin-responsive GLUT4 storage vesicles isolated from 3T3–L1 adipocytes. Mol. Cell. Biol. *20*, 416–427.

Haucke, V., and De Camilli, P. (1999). AP-2 recruitment to synaptotagmin stimulated by tyrosine-based endocytic motifs. Science *285*, 1268–1271.

Herman, G.A., Bonzelius, F., Cieutat, A.M., and Kelly, R.B. (1994). A distinct class of intracellular storage vesicles, identified by expression of the glucose transporter GLUT4. Proc. Natl. Acad. Sci. USA *91*, 12750–12754.

Holroyd, C., Kistner, U., Annaert, W., and Jahn, R. (1999). Fusion of endosomes involved in synaptic vesicle recycling. Mol. Biol. Cell *10*, 3035–3044.

James, D.E., Brown, R., Navarro, J., and Pilch, P.F. (1988). Insulin-regulatable tissues express a unique insulin-sensitive glucose transport protein. Nature *333*, 183–185.

James, D.E., Lederman, L., and Pilch, P.F. (1987). Purification of insulin-dependent exocytic vesicles containing the glucose transporter. J. Biol. Chem. *262*, 11817–11824.

Johnson, A.O., Subtil, A., Petrush, R., Kobylarz, K., Keller, S.R., and McGraw, T.E. (1998). Identification of an insulin-responsive, slow endocytic recycling mechanism in Chinese hamster ovary cells. J. Biol. Chem. *273*, 17968–17977.

Jones, A.T., and Wessling-Resnick, M. (1998). Inhibition of in vitro endosomal vesicle fusion activity by aminoglycoside antibiotics. J. Biol. Chem. *273*, 25301–25309.

Kahn, B.B. (1998). Type 2 diabetes: when insulin secretion fails to compensate for insulin resistance. Cell *92*, 593–596.

Kahn, R.A., Yucel, J.K., and Malhotra, V. (1993). ARF signaling: a potential role for phospholipase D in membrane traffic [comment]. Cell *75*, 1045–1048.

Kanai, F., Nishioka, Y., Hayashi, H., Kamohara, S., Todaka, M., and Ebina, Y. (1993). Direct demonstration of insulin-induced GLUT4 translocation to the surface of intact cells by insertion of a c-myc epitope into an exofacial GLUT4 domain. J. Biol. Chem. *268*, 14523–14526.

Kandror, K.V., Coderre, L., Pushkin, A.V., and Pilch, P.F. (1995). Comparison of glucose-transporter–containing vesicles from rat fat and muscle tissues: evidence for a unique endosomal compartment. Biochem. J. *307*, 383–390.

Kandror, K.V., and Pilch, P.F. (1994). gp160, a tissue-specific marker for insulin-activated glucose transport. Proc. Natl. Acad. Sci. USA *91*, 8017–8021.

Keller, S.R., Scott, H.M., Mastick, C.C., Aebersold, R., and Lienhard, G.E. (1995). Cloning and characterization of a novel insulin-regulated membrane aminopeptidase from Glut4 vesicles [published erratum appears in J. Biol. Chem. (1995) *270*, 30236]. J. Biol. Chem. *270*, 23612–23618.

Kirchhausen, T., Bonifacino, J.S., and Riezman, H. (1997). Linking cargo to vesicle formation: receptor tail interactions with coat proteins. Curr. Opin. Cell Biol. *9*, 488–495.

Kishore, B.K., Lambricht, P., Laurent, G., Maldague, P., Wagner, R., and Tulkens, P.M. (1990). Mechanism of protection afforded by polyaspartic acid against gentamicin-induced phospholipidosis. II. Comparative in vitro and in vivo studies with poly-L-aspartic, poly-L-glutamic and poly-D-glutamic acids. J. Pharmacol. Exp. Ther. *255*, 875–885.

Ktistakis, N.T., Brown, H.A., Waters, M.G., Sternweis, P.C., and Roth, M.G. (1996). Evidence that phospholipase D mediates ADP ribosylation factor-dependent formation of Golgi coated vesicles. J. Cell Biol. *134*, 295–306.

Kuehn, M.J., Herrmann, J.M., and Schekman, R. (1998). COPII-cargo interactions direct protein sorting into ER-derived transport vesicles. Nature *391*, 187–190.

Lee, W., Ryu, J., Souto, R.P., Pilch, P.F., and Jung, C.Y. (1999). Separation and partial characterization of three distinct intracellular GLUT4 compartments in rat adipocytes: subcellular fractionation without homogenization. J. Biol. Chem. *274*, 37755–37762.

Lichtenstein, Y., Desnos, C., Faúndez, V., Kelly, R.B., and Clift-O'Grady, L. (1998). Vesiculation and sorting from PC12-derived endosomes in vitro. Proc. Natl. Acad. Sci. USA *95*, 11223–11228.

Lippincott-Schwartz, J., Yuan, L., Tipper, C., Amherdt, M., Orci, L., and Klausner, R.D. (1991). Brefeldin A's effects on endosomes, lysosomes, and the TGN suggest a general mechanism for regulating organelle structure and membrane traffic. Cell *67*, 601–616.

Liscovitch, M., Chalifa, V., Pertile, P., Chen, C.S., and Cantley, L.C. (1994). Novel function of phosphatidylinositol 4,5-bisphosphate as a cofactor for brain membrane phospholipase D. J. Biol. Chem. *269*, 21403–21406.

Livingstone, C., James, D.E., Rice, J.E., Hanpeter, D., and Gould, G.W. (1996). Compartment ablation analysis of the insulin-responsive glucose transporter (GLUT4) in 3T3–L1 adipocytes. Biochem. J. *315*, 487–495.

Malide, D., Dwyer, N.K., Blanchette-Mackie, E.J., and Cushman, S.W. (1997). Immunocytochemical evidence that GLUT4 resides in a specialized translocation post-endosomal VAMP2-positive compartment in rat adipose cells in the absence of insulin. J. Histochem. Cytochem. *45*, 1083–1096.

Martin, S., Rice, J.E., Gould, G.W., Keller, S.R., Slot, J.W., and James, D.E. (1997). The glucose transporter GLUT4 and the aminopeptidase vp165 colocalise in tubulo-vesicular elements in adipocytes and cardiomyocytes. J. Cell Sci. *110*, 2281–2291.

Martin, S., Tellam, J., Livingstone, C., Slot, J.W., Gould, G.W., and James, D.E. (1996). The glucose transporter (GLUT-4) and vesicle-associated membrane protein-2 (VAMP-2) are segregated from recycling endosomes in insulin-sensitive cells. J. Cell Biol. *134*, 625–635.

Mayor, S., Presley, J.F., and Maxfield, F.R. (1993). Sorting of membrane components from endosomes and subsequent recycling to the cell surface occurs by a bulk flow process. J. Cell Biol. *121*, 1257–1269.

McGraw, T.E., Greenfield, L., and Maxfield, F.R. (1987). Functional expression of the human transferrin receptor cDNA in Chinese hamster ovary cells deficient in endogenous transferrin receptor. J. Cell Biol. *105*, 207–214.

McMahon, H.T., Ushkaryov, Y.A., Edelmann, L., Link, E., Binz, T., Niemann, H., Jahn, R., and Südhof, T.C. (1993). Cellubrevin is a ubiquitous tetanus-toxin substrate homologous to a putative synaptic vesicle fusion protein [see comments]. Nature *364*, 346–349.

Mellman, I. (1996). Endocytosis and molecular sorting. Annu. Rev. Cell Dev. Biol. *12*, 575–625.

Mellman, I., and Warren, G. (2000). The road taken: past and future foundations of membrane traffic. Cell *100*, 99–112.

Mu, F.T., Callaghan, J.M., Steele-Mortimer, O., Stenmark, H., Parton, R.G., Campbell, P.L., McCluskey, J., Yeo, J.P., Tock, E.P., and Toh, B.H. (1995). EEA1, an early endosome-associated protein: EEA1 is a conserved alpha-helical peripheral membrane protein flanked by cysteine "fingers" and contains a calmodulin-binding IQ motif. J. Biol. Chem. *270*, 13503–13511.

Plemper, R.K., and Wolf, D.H. (1999). Retrograde protein translocation: ERADication of secretory proteins in health and disease. Trends. Biochem. Sci. *24*, 266–270.

Prekeris, R., Klumperman, J., Chen, Y.A., and Scheller, R.H. (1998). Syntaxin 13 mediates cycling of plasma membrane proteins via tubulovesicular recycling endosomes. J. Cell Biol. *143*, 957–971.

Ramm, G., Slot, J.W., James, D.E., Stoorvogel, W. (2000). Insulin recruits GLUT4 from specialized VAMP2-carrying vesicles as well as from the dynamic endosomal/trans-Golgi network in rat adipocytes. Mol. Biol. Cell *11*, 4079–4091.

Randazzo, P.A., Weiss, O., and Kahn, R.A. (1992). Preparation of recombinant ADP-ribosylation factor. Methods Enzymol. *219*, 362–369.

Rodnick, K.J., Slot, J.W., Studelska, D.R., Hanpeter, D.E., Robinson, L.J., Geuze, H.J., and James, D.E. (1992). Immunocytochemical and biochemical studies of GLUT4 in rat skeletal muscle. J. Biol. Chem. *267*, 6278–6285.

Ross, S.A., Keller, S.R., and Lienhard, G.E. (1998). Increased intracellular sequestration of the insulin-regulated aminopeptidase upon differentiation of 3T3–L1 cells. Biochem. J. *330*, 1003–1008.

Ross, S.A., Scott, H.M., Morris, N.J., Leung, W.Y., Mao, F., Lienhard, G.E., and Keller, S.R. (1996). Characterization of the insulin-regulated membrane aminopeptidase in 3T3–L1 adipocytes. J. Biol. Chem. *271*, 3328–3332.

Salem, N., Faúndez, V., Horng, J.T., and Kelly, R.B. (1998). A v-SNARE participates in synaptic vesicle formation mediated by the AP3 adaptor complex. Nat. Neurosci. *1*, 551–556.

Sheff, D.R., Daro, E.A., Hull, M., and Mellman, I. (1999). The receptor recycling pathway contains two distinct populations of early endosomes with different sorting functions. J. Cell Biol. *145*, 123–139.

Slot, J.W., Geuze, H.J., Gigengack, S., James, D.E., and Lienhard, G.E. (1991a). Translocation of the glucose transporter GLUT4 in cardiac myocytes of the rat. Proc. Natl. Acad. Sci. USA *88*, 7815–7819.

Slot, J.W., Geuze, H.J., Gigengack, S., Lienhard, G.E., and James, D.E. (1991b). Immuno-localization of the insulin regulatable glucose transporter in brown adipose tissue of the rat. J. Cell Biol. *113*, 123–135.

Smith, R.M., Charron, M.J., Shah, N., Lodish, H.F., and Jarett, L. (1991). Immunoelectron microscopic demonstration of insulin-stimulated translocation of glucose transporters to the plasma membrane of isolated rat adipocytes and masking of the carboxyl-terminal epitope of intracellular GLUT4. Proc. Natl. Acad. Sci. USA *88*, 6893–6897.

Sönnichsen, B., De Renzis, S., Nielsen, E., Rietdorf, J., and Zerial, M. (2000). Distinct membrane domains on endosomes in the recycling pathway visualized by multicolor imaging of Rab4, Rab5, and Rab11. J. Cell Biol. *149*, 901–914.

Springer, S., and Schekman, R. (1998). Nucleation of COPII vesicular coat complex by endoplasmic reticulum to Golgi vesicle SNAREs. Science *281*, 698–700.

Springer, S., Spang, A., and Schekman, R. (1999). A primer on vesicle budding. Cell *97*, 145–148.

Stoorvogel, W., Oorschot, V., and Geuze, H.J. (1996). A novel class of clathrin-coated vesicles budding from endosomes. J. Cell Biol. *132*, 21–33.

Tooze, J., and Hollinshead, M. (1992). In AtT20 and HeLa cells brefeldin A induces the fusion of tubular endosomes and changes their distribution and some of their endocytic properties. J. Cell Biol. *118*, 813–830.

Ullrich, O., Reinsch, S., Urbé, S., Zerial, M., and Parton, R.G. (1996). Rab11 regulates recycling through the pericentriolar recycling endosome. J. Cell Biol. *135*, 913–924.

van der Sluijs, P., Hull, M., Webster, P., Mâle, P., Goud, B., and Mellman, I. (1992). The small GTP-binding protein rab4 controls an early sorting event on the endocytic pathway. Cell *70*, 729–740.

Wei, M.L., Bonzelius, F., Scully, R.M., Kelly, R.B., and Herman, G.A. (1998). GLUT4 and transferrin receptor are differentially sorted along the endocytic pathway in CHO cells. J. Cell Biol. *140*, 565–575.

West, M.A., Bright, N.A., and Robinson, M.S. (1997). The role of ADP-ribosylation factor and phospholipase D in adaptor recruitment. J. Cell Biol. *138*, 1239–1254.

White, S., Miller, K., Hopkins, C., and Trowbridge, I.S. (1992). Monoclonal antibodies against defined epitopes of the human transferrin receptor cytoplasmic tail. Biochim. Biophys. Acta *1136*, 28–34.

Whitney, J.A., Gomez, M., Sheff, D., Kreis, T.E., and Mellman, I. (1995). Cytoplasmic coat proteins involved in endosome function [see comments]. Cell *83*, 703–713.

Yamashiro, D.J., Tycko, B., Fluss, S.R., and Maxfield, F.R. (1984). Segregation of transferrin to a mildly acidic (pH 6.5) para-Golgi compartment in the recycling pathway. Cell *37*, 789–800.-